Order-Chaos-Order Transitions in Electrosprays: The Electrified Dripping Faucet

Ioan Marginean, Peter Nemes, and Akos Vertes*

Department of Chemistry, The George Washington University, Washington, DC 20052, USA

(Received 24 February 2006; published 9 August 2006)

Electrosprays have diverse applications including protein analysis, electrospinning, and nanoencapsulation for drug delivery. We show that a variety of electrospray regimes exhibit fundamental analogy with the nonlinear dynamics of a dripping faucet. The applied voltage in electrosprays results in additional period doublings and temporal order-chaos-order transitions. Attractors in the return maps show logarithmic self-similarity in time, suggesting self-similar capillary waves on the meniscus. The bifurcations in ejection time can be explained by phase variations between capillary waves and pinch-off conditions and by ejection mode changes due to contact angle variations.

DOI: 10.1103/PhysRevLett.97.064502 PACS numbers: 47.65.−d, 47.20.Ky, 47.52.+j, 47.55.db

Electrosprays have diverse applications including protein analysis [1], electrospinning, steering of microsatellites in space, and nanoencapsulation for drug delivery. Theoretical studies of the initial droplet production in electrostatic spraying focus mainly on the effect of the electric field on drop formation [2] and on the breakup of the charged jet [3]. In these studies the interaction of the liquid meniscus with the end of the dispensing capillary is ignored. Even in studies where the capillary is present in the description, the interaction energy is neglected through the assumption of infinitely thin capillary wall. This approximation does not always hold up in electrospray formation where the dynamics of detachment from the capillary can be comparable in energy to the capillary-gravitational waves on the meniscus.

The dripping faucet problem is a well-known example in nonlinear dynamics because, in a simple system, it exhibits consecutive period doublings resulting in temporal order-chaos transitions [4,5]. In this Letter we demonstrate that certain modes of electrospraying exhibit a fundamental analogy with dripping faucets with some important distinctions. Applying high voltage to a leaky ''faucet'' (i.e., an electrospray capillary) makes this problem more complex because the Maxwell stress produced in the liquid overtakes gravitational forcing, modifies the dripping behavior, and eventually produces an electrospray. This complexity gives rise to a fascinating variety of spraying regimes, unique to electrosprays, including spindle, pulsating Taylor cone, cone-jet, and multijet emission modes [6]. Based on detailed spray current measurements, a systematic classification of three axisymmetric emission modes was established [7]. Changes between these modes are reported to exhibit aperiodic behavior [8], but detailed analysis of the transition dynamics is lacking.

Recently, we have shown that for a pulsating Taylor cone (axial mode II) a circular nodal line is present demonstrating the existence of long wavelength capillary waves on the electrified meniscus [9]. Because of the accumulation of surface charge, these waves occasionally give way to the detachment of macroscopic liquid volumes. Three distinct emission modes, droplet, spindle, and jet, were reported for a resting droplet placed in a strong electric field [10].

In this Letter, we examine the temporal characteristics of the burst mode (axial mode I), the most complex of the axial regimes, that exhibits nested oscillations. The emergence of this mode from simple dripping is followed as a function of high voltage for high and low conductivity ionic solutions. We explore how the presence of electric field affects period doubling and order-chaos-order transitions as the system approaches axial mode II.

The results presented in this Letter were obtained using the methods described in our previous publications [8,9]. Briefly, a syringe pump was used to supply aqueous methanol solutions at various flow rates through stainless steel capillaries. The needles included tapered tip $od/id = 320/100\ \mu\mathrm{m}/\mu\mathrm{m}$ and blunt tip 510/260, 460/260, 470/130, 360/180, 260/130 $\mu\mathrm{m}/\mu\mathrm{m}$ geometries. The current on a flat stainless steel counter electrode (placed $d = 12$–30 mm away from the tip of the capillary) was captured by a digital oscilloscope. Sudden changes in the spray current were utilized as a source of trigger for fast imaging. The oscilloscope trigger was sent directly to a delay generator that, in turn, triggered a fast digital camera. The results presented in this Letter were obtained with 50% methanol (low conductivity) and 1% acetic acid in 50% methanol (high conductivity) solutions with electrical conductivities, σ, of 3.5 μS/cm and 117.1 μS/cm, respectively.

To capture the ejection modes and their transitions, spray current data were collected at different voltage settings for 10 s. Typical spray current measurements for axial mode I are presented in Fig. 1. The insets show time-lapse images associated with the emission of a jet and two droplets through jetting spindles during a burst [Fig. 1(a)] and individual jets related to the first and tenth current spike of an 18-jet burst [Fig. 1(b)].

The relative strength of electrostatic and capillary forces is expressed by the electric Bond number, $\mathrm{Bo}_E = rE^2/\gamma$, where E is the electric field, r is the characteristic length, typically the radius of the capillary, and γ is the surface tension of the liquid. For these conductive liquids, from the

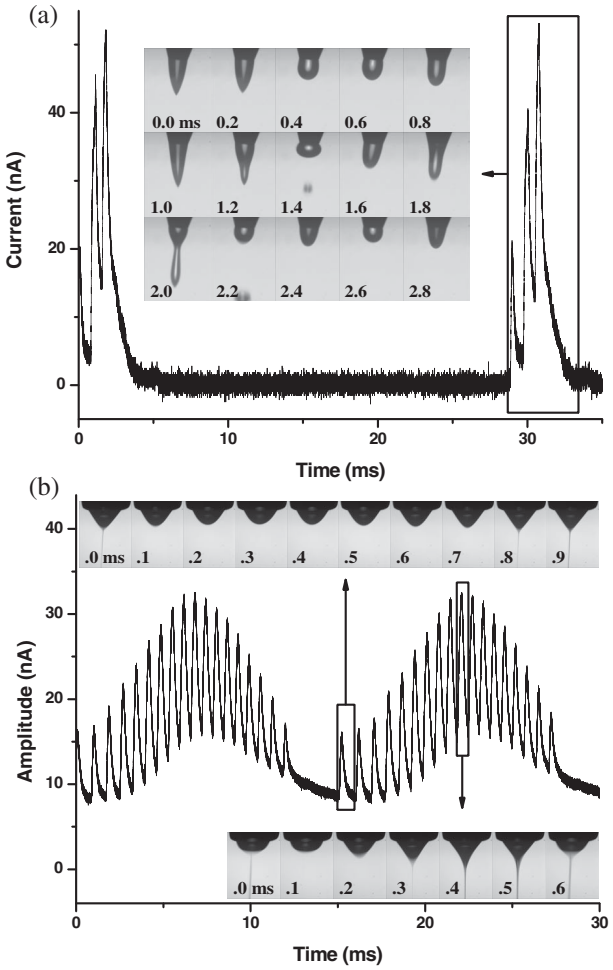

FIG. 1. Current measurements for electrosprays in axial mode I (burst regime): (a) various ejection modes from needle (tapered tip) spraying 1% acetic acid in 50% MeOH at 1915 V capillary voltage and 1 μl/min ($d = 12$ mm); (b) repeated jet ejection from needle (blunt tip), spraying 50% MeOH at 3000 V and 4 μl/min ($d = 30$ mm). Insets depict snapshot sequences during boxed period captured at times indicated in each frame.

perspective of electric field distributions, one can approximate the capillary and the protruding liquid jointly as a point facing a plane counter electrode. The corresponding electric field distribution is $E = 2U/[r \ln(4d/r)]$, where U is the applied potential and d is the distance from the tip of the capillary to the counterelectrode. The electric Bond number calculated for this system is a quadratic function of the applied potential and grows with decreasing capillary radius. For the systems in Fig. 1(a) and 1(b) the values are $\mathrm{Bo}_E = 1.55$ and $\mathrm{Bo}_E = 0.97$, respectively. These numbers indicate a comparable effect of the electric and capillary forces and are below the onset of steady jetting (axial mode III).

For a resting droplet, the behavior of the liquid meniscus is determined by the value of Bo_E and the contact angle, α, at the capillary tip. According to shape measurements, for perfectly conducting droplets attached to a surface there are three possible scenarios [10]. In the low field limit with capillarity dominating, steady state droplet shapes are formed. At higher electric fields and low contact angles $\alpha < 0.8\pi$ jetting is observed, whereas at $0.8\pi < \alpha < \pi$ the entire droplet resembling a spindle is dislodged. In our systems, however, the droplet at the end of the capillary is not at rest; its shape and the contact angle vary with time. Nevertheless, we observed both jetting and the departure of entire spindlelike droplets.

For an oscillating meniscus supplied with liquid through a capillary, the dynamics is very complex and the conditions determined for resting droplets are not directly applicable. This complexity stems from the interaction between the fluid flow, interfacial dynamics, and electric polarization. For a perfectly conducting liquid, it is expected that the (Oh, We, Bo_E) parameter space, where Oh and We are the Ohnesorge and Weber number, respectively, can be partitioned into domains with distinct ejection modes. For imperfect conductors, however, the charge and hydrodynamic relaxation may become linked. Indeed, even for the high conductivity solution in our study, the charge-relaxation time, $\tau_C = \epsilon/(4\pi\sigma)$, and the hydrodynamic relaxation time, $\tau_H = \eta r/\gamma$, where η is the viscosity, are comparable, i.e., 3.8 μs and 2.5 μs, respectively. For the low conductivity case, $\tau_C = 129$ μs and $\tau_H = 3.1$ μs; thus, the charge redistribution significantly lags behind the mechanical deformation. This is known to strongly affect the dispersion relation of capillary waves and result in enhanced instability, i.e., in the onset of liquid ejection at lower field values [11,12].

The deformation of the liquid meniscus into a sharp point influences both the electric field and the local value of the electric Bond number. For example, a conical liquid protrusion with a 1 μm radius of curvature at the tip results in local values of $\mathrm{Bo}_E = 31.4$ for Fig. 1(a) and $\mathrm{Bo}_E = 65.5$ for Fig. 1(b). Thus, in both cases the electric forces dominate and jetting ensues. Indeed, in the insets of the two panels of Fig. 1 jetting can be observed. The difference in conductivity, however, results in dissimilar dynamics and consequently the liquid ejection events within the bursts are quite different. After jet ejection in the first two frames (0.0 ms and 0.2 ms) of Fig. 1(a), we observed the formation of a spindlelike jetting meniscus (1.0–1.2 ms) and the departure of a droplet (1.4 ms). Another jetting spindle formation (2.0 ms) and another droplet ejection (2.2 ms) follow. At this point a sufficient amount of charge is removed for the surface tension to take control. The burst is over and the meniscus recedes through oscillatory motion. Figure 1(b), however, represents a different scenario. In this sequence, the jet ejection repeats itself throughout the burst until sufficient charge is removed.

As demonstrated above, the expulsion of charged liquid can proceed through the departure of droplets including ones resembling a spindle, as well as through jet ejection. These modes of liquid removal are associated with divergent surface deformations of greatly different wavelengths. In case of droplet or spindle removal, the wavelength of the divergent mode is commensurate with the capillary diame-

ter because all these waves are bound by the liquid contact line at the tip. The frequency spectrum of these oscillations for a perfectly conducting sphere is known from the work of Rayleigh [13]. The formation of a thin jet, however, is linked to the divergence of a much shorter wavelength mode. These perturbations originate from thermal surface fluctuations of amplitude $(kT/\gamma)^{1/2}$ and exponentially grow into a filament of microscopic diameter. In the first order, this diameter is determined by the condition that the local Bond number exceeds a critical value, $\mathrm{Bo}_E > \mathrm{Bo}_E^*$. For static menisci, the critical Bond number decreases from $\mathrm{Bo}_E^* \approx 5.14$ at static contact angle $\alpha_s = \pi/2$ at the capillary surface to $\mathrm{Bo}_E^* \approx 1.21$ at $\alpha_s = 0.8\pi$ [10]. The dependence of the critical Bond number on the contact angle points to the important and largely unexplored connection between the shape and surface properties of the capillary and the spraying regimes in electrosprays. For dynamic menisci observed in electrosprays, the contact angle is a function of time due to the shape changes of the meniscus stemming from their oscillation and from the gradual accumulation of liquid (see the insets in Fig. 1).

It is worth noting that even within a burst the time intervals between ejection events are not constant. In Fig. 1(a), the time between the first and the second peak in the spray current is longer than the period between the second and the third. Similarly, in Fig. 1(b) the lengths of ejection intervals within a burst go through a minimum. Variations in these time intervals, and eventually a change in the spraying mode, can be induced by altering the liquid flow rate or the high voltage. Here we present the transitions induced by high voltage changes.

Ejection intervals were analyzed in a long time series (100 s) corresponding to conditions in Fig. 1(a). As the high voltage (and with it the electric Bond number) increased from 1880 V, period doubling (1890 V), i.e., a bifurcation, and tripling (1905 V) was observed [14]. At 1920 V, additional bifurcations resulted in close to chaotic behavior, but further increasing the voltage to 1935 V led to a sudden transition to a pulsating Taylor cone, characterized by a single period. The observed order-chaos-order transition is specific to electrosprays and in the absence of electric field, i.e., for a dripping faucet, it does not exist. Increasing the flow rate for a chaotic dripping faucet typically results in the onset of jetting.

To examine the ejection intervals of the two sprays in Fig. 1, return maps were constructed (see Fig. 2). Plotting the time interval between peaks n and $n+1$, T_{n+1}, as a function of the previous period, T_n, the voltage-induced transitions can be clearly followed. In the high conductivity case [Fig. 2(a)] one can identify a period-4 attractor in the 1880 V panel, which morphs into an L-shaped attractor at 1885 V and almost disappears at 1900 V. The onset of the burst regime introduces three more attractors that are shifted to shorter time periods. The onset of the axial II regime at 1935 V produces a single attractor corresponding to the Taylor cone pulsation period. These transitions

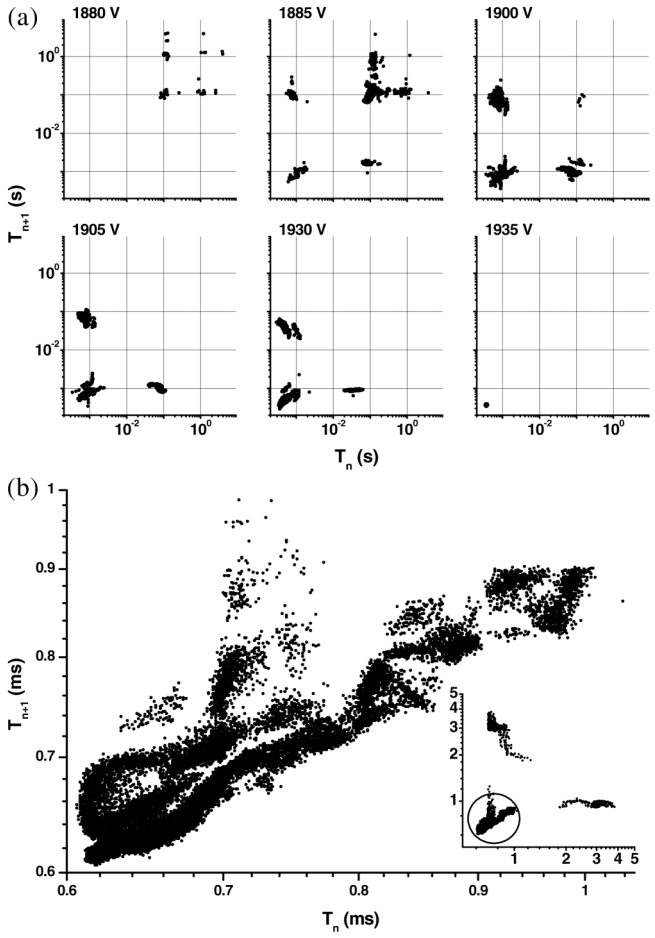

FIG. 2. Return maps for spray current measured for: (a) high conductivity and (b) low conductivity solutions. Conditions were identical to those in corresponding panels of Fig. 1.

resemble the behavior of the dripping faucet at increasing flow rates [15]. In a significant departure from the linear return maps for dripping faucets, however, for electrosprays the characteristic time periods span over 3 orders of magnitude and the return maps are logarithmic.

The symmetry of period-4 attractors shown in the 1880 and 1900 V panels suggests that the temporal behavior of axial mode I electrosprays is logarithmically self-similar. Increasing the spray voltage from 1880 V by only 20 V shifts the period-4 attractor to time scales that are 2 orders of magnitude shorter. At the same time, the disparity between low and high frequency oscillations doubles on a logarithmic scale. It has been demonstrated that the temporal periodicity reflected in the return maps is the consequence of capillary waves on the liquid meniscus [9]. Through the dispersion relation of the capillary waves the logarithmic self-similarity in time translates into logarithmic self-similarity in space. Thus, the wavelengths of the corresponding divergent capillary waves on the electrified meniscus are also expected to be dramatically different.

Figure 2(b) illustrates the return map corresponding to the current measurement for the low conductivity case

presented in Fig. 1(b). Since after a relatively long pause between two bursts a shorter period between peaks within the same burst follows, the first peak in a burst is always represented by a point in the rightmost attractor. As the time between consecutive peaks gets shorter, the point travels along the strange attractor following a path below the main diagonal. Upon reaching the shorter times, the point moves erratically several times before it leaves the attractor at the top of the main diagonal. This signifies the increase in periods between consecutive peaks toward the end of the burst. Finally, at the last ejection in the burst the point jumps to the top attractor indicating the beginning of a new cycle.

Analysis of the nonlinear capillary oscillations for a flat surface of a poorly conducting liquid indicates that, for these systems, additional instability is induced by the aperiodic charge-relaxation [12]. This is in contrast to the findings for high conductivity liquids, where the instability is produced by the capillary waves. Indeed, comparing the insets in Fig. 1(a) (high conductivity case) and Fig. 1(b) (low conductivity case) reveals this difference. While in Fig. 1(a) the droplet shape changes show the oscillations characteristic of capillary waves, in Fig. 1(b) most of these waves are damped and the shape changes follow the dynamics of monotonic charge rearrangement toward the tip of the Taylor cone. The aperiodic behavior induced by charge relaxation in low conductivity systems is evidenced in Fig. 2(b). The strange attractor in this figure is a result of the added instability due to this aperiodic behavior.

Similar to the case of a dripping faucet, a phase-based explanation of period doubling [5] can be provided for liquid ejection in electrosprays. After the excess charge is expelled, the surface tension regains control and the tip of the cone recoils, transmitting a wave radially toward the circular contact line between needle and liquid. At the boundary the wave bounces, pushing the liquid back into conical shape and creating the conditions for a new liquid ejection process. The momentum of the liquid being pumped through the capillary and the increasing tangential stress due to the continually accumulating charge also promote the return to conical shape. The surface tension may be able to contain the liquid in oscillatory motion and the wave diminishes traveling back and forth on the meniscus. This explains the electrospray behavior in the dripping mode. In this mode the electric Bond number is less than or comparable to the gravitational Bond number, Bo_G, and the electrospray approaches a dripping faucet. In axial mode I, Bo_E exceeds Bo_G. Depending on the phase of the capillary wave, pinch off can occur when Bo_G (dripping mode) or Bo_E (burst mode) is sufficiently close to the critical value.

The phase-based rationalization of bifurcations in ejection time and the one based on ejection mode changes due to contact angle variations complement each other. They emphasize two different aspects of the electrospray, electrically enhanced nonlinear capillary waves on the meniscus and the capillary liquid interactions. A unified treatment accounting for both of these factors is needed for a more complete description of electrosprays.

In most applications, but especially in electrospray ionization for protein analysis and in nanoencapsulation through composite sprays, the stability of a selected spraying mode is essential. Compared to the pulsating modes, in cone-jet mode the efficiency of ion production increases by an order of magnitude. In nanoencapsulation the formation of a steady coaxial jet of immiscible liquids is a prerequisite for the successful production of nanoscopic capsules. Our results provide a new understanding of how spraying mode changes occur and what can be done to avoid them. By monitoring and analyzing the spray current, a feedback mechanism can be established to stabilize the spray through counteracting voltage or flow rate changes.

This material is based upon work supported by the National Science Foundation under Grant No. 0415521 and in part by the Department of Energy under Grant No. DE-FG02-01ER15129.

*Corresponding author.
Email address: vertes@gwu.edu

[1] J. B. Fenn, M. Mann, C. K. Meng, S. F. Wong, and C. M. Whitehouse, Science **246**, 64 (1989).
[2] H. A. Stone, J. R. Lister, and M. P. Brenner, Proc. R. Soc. A **455**, 329 (1999).
[3] J. M. Lopez-Herrera and A. M. Ganan-Calvo, J. Fluid Mech. **501**, 303 (2004).
[4] B. Ambravaneswaran, H. J. Subramani, S. D. Phillips, and O. A. Basaran, Phys. Rev. Lett. **93**, 034501 (2004).
[5] P. Coullet, L. Mahdevan, and C. S. Riera, J. Fluid Mech. **526**, 1 (2005).
[6] M. Cloupeau and B. Prunet-Foch, J. Aerosol Sci. **25**, 1021 (1994).
[7] R. Juraschek and F. W. Röllgen, Int. J. Mass Spectrom. **177**, 1 (1998).
[8] L. Parvin, M. C. Galicia, J. M. Gauntt, L. M. Carney, A. B. Nguyen, E. Park, L. Heffernan, and A. Vertes, Anal. Chem. **77**, 3908 (2005).
[9] I. Marginean, L. Parvin, L. Heffernan, and A. Vertes, Anal. Chem. **76**, 4202 (2004).
[10] S. N. Reznik, A. L. Yarin, A. Theron, and E. Zussman, J. Fluid Mech. **516**, 349 (2004).
[11] J. R. Melcher and C V. Smith, Jr., Phys. Fluids **12**, 778 (1969).
[12] S. O. Shiryaeva, A. I. Grogor'ev, and V. A. Koromyslov, Tech. Phys. **42**, 884 (1997).
[13] L. Rayleigh, Philos. Mag. **14**, 184 (1882).
[14] I. Marginean, Ph.D. thesis, The George Washington University, 2006.
[15] B. Ambravaneswaran, S. D. Phillips, and O. A. Basaran, Phys. Rev. Lett. **85**, 5332 (2000).